

Synthesis, Characterization and Structural Studies on the First Rhenium Complex with Di(2-pyridyl) Ketone 2,4-Dinitrophenylhydrazone (dpkdnph), *fac*-[Re(CO)₃(dpkdnph)Cl]

Mohammed Bakir^[a]

Keywords: Rhenium / Carbonyl ligands / Hydrazones

When di(2-pyridyl) ketone 2,4-dinitrophenylhydrazone (dpkdnph) was allowed to react with [Re(CO)₅Cl] in refluxing toluene *fac*-[Re(CO)₃(dpkdnph)Cl] was formed in good yield. Spectroscopic measurements on *fac*-[Re(CO)₃(dpkdnph)Cl] revealed strong solvent dependence as manifested by the high sensitivity of its electronic absorption spectra to solvent variation. Electrochemical measurements on *fac*-[Re(CO)₃(dpkdnph)Cl] in DMF show electrochemical properties with quasi-reversible reductions following an irreversible one-electron transfer. Structural studies on a brown

crystal of *fac*-[Re(CO)₃(dpkdnph)Cl]·CH₃CN grown from an acetonitrile solution of *fac*-[Re(CO)₃(dpkdnph)Cl] show well separated linear CH₃CN and pseudo-octahedral *fac*-[Re(CO)₃(dpkdnph)Cl], with the major distortion about rhenium being due to the bidentate binding of dpkdnph to form a six-membered Re–N–C–C–N metallacyclic ring in a boat conformation. The molecular packing shows a web of *fac*-[Re(CO)₃(dpkdnph)Cl]·CH₃CN units interlocked via a network of intra- and intermolecular non-covalent interactions that include donor/acceptor and hydrogen bonds.

Introduction

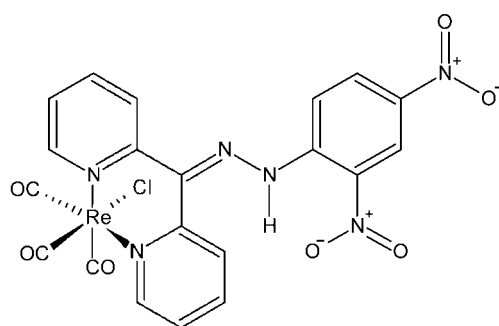
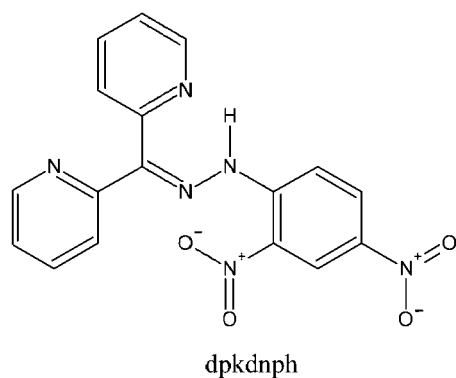
Hydrazones and their compounds have been extensively studied for their rich physicochemical properties, reactivity patterns and applications in many important chemical processes that include non-linear optics, medicine, molecular sensing and separations.^[1–16] The synthesis and characterization of rhenium carbonyl compounds of di(2-pyridyl) ketone (dpk), di(2-pyridyl)amine (dpa), di(2-pyridyl) ketone oxime (dpk.oxime), and di(2-pyridyl) ketone *p*-nitrophenyl hydrazone (dpknph) were described by us previously.^[17–20] Electrochemical measurements on *fac*-[Re(CO)₃(dpk)Cl] and *fac*-[Re(CO)₃(dpk.oxime)Cl] revealed strong solvent dependence and the possible use of *fac*-[Re(CO)₃(dpk)Cl] as an electrochemical sensor for electrophiles that include metal ions.^[17–19] Optical and thermodynamic measurements in polar solvents on dpknph and *fac*-[Re(CO)₃(dpknph)Cl] show the presence of two charge-transfer bands for the free ligand and its metal compound; the electronic/charge transfer in *fac*-[Re(CO)₃(dpknph)Cl] is faster than that in dpknph, and therefore *fac*-[Re(CO)₃(dpknph)Cl] can be used as a spectrophotometric sensor for metal ions.^[20,21] These results prompted us to explore how a variation in the ligand backbone affects the electrochemical and optical properties of the complex, and here I report the synthesis, characterization and solid-state structure of the first metal compound of di(2-pyridyl) ketone 2,4-dinitrophenyl hydrazone (dpkdnph). Although a variety of

2,4-dinitrophenylhydrazones have been reported, to the best of my knowledge there has been no report on the isolation of dpkdnph.^[1]

Results and Discussion

The reaction between [Re(CO)₅Cl] and dpkdnph in toluene under reflux gave *fac*-[Re(CO)₃(dpkdnph)Cl] in good yield. This reaction is similar to those reported for the synthesis of *fac*-[Re(CO)₃(L-L)Cl] (L-L = dpk, dpk.oxime, dpknph) from [Re(CO)₅Cl] and L-L in refluxing toluene.^[17–20] The formulation of the isolated rhenium-carbonyl as *fac*-[Re(CO)₃(dpkdnph)Cl] is based on the results of a number of spectroscopic measurements and a comparison of these results with those reported for *fac*-[Re(CO)₃(L-L)Cl].^[17–20] In the IR spectrum of *fac*-[Re(CO)₃(dpkdnph)Cl] three strong bands appeared in the ν(C=O) stretching region similar to those observed for *fac*-[Re(CO)₃(dpknph)Cl] and other tricarbonylhalorhenium(I) compounds with polypyridyl-like ligands, thus confirming the assigned *fac* geometry.^[17–20] The ν(C=N) absorption of the hydrazone moiety and the combined ν(C=C) and ν(C=N) of the pyridine vibrations are normal and in the same region as in *fac*-[Re(CO)₃(dpknph)Cl].^[20] A single absorption band was observed for the ν(NH) stretching mode signalling a free N–H in the solid state.^[22] The ¹H NMR spectrum of *fac*-[Re(CO)₃(dpkdnph)Cl] (see Exp. Sect.) is solvent dependent, indicating a solvent-solute interaction. No evidence of paramagnetic line broadening or unusual shifts of resonances appeared in the spectra of this compound, thus confirming its diamagnetic character.

^[a] Department of Chemistry, The University of the West Indies-Mona Campus, Kingston 7, Jamaica, W. I.



The electronic absorption spectra of *fac*-[Re(CO)₃(dpkdnph)Cl] show spectral features similar to those reported for *fac*-[Re(CO)₃(dpknp)Cl], although subtle differences are apparent.^[20,21] The charge-transfer bands in *fac*-[Re(CO)₃(dpkdnph)Cl] shift to high-energy relative to *fac*-[Re(CO)₃(dpknp)Cl] due to a decrease in the electron-withdrawing ability of dpkdnph compared to dpknp. In non-polar solvents such as CH₂Cl₂ a highly intense high-energy charge-transfer band appeared (Figure 1a), in polar solvents such as CH₃CN two charge-transfer bands appeared (Figure 1b), and in highly polar solvents such as DMF a low-energy charge-transfer band appeared (Figure 1c). The intensity and location of these bands are solvent dependent. The gradual addition of a physical or chemical stimulus to a solution of *fac*-[Re(CO)₃(dpkdnph)Cl] causes an interconversion between the low- and high-energy intra-ligand charge-transfer bands of *fac*-[Re(CO)₃(dpkdnph)Cl]. For example, when a DMF solution of *fac*-[Re(CO)₃(dpkdnph)Cl] was exposed to sunlight, the intensity of the low-energy charge-transfer band decreased and the intensity of the high-energy band increased (Figure 2). The spectrophotometric response of *fac*-[Re(CO)₃(dpkdnph)Cl] towards physical and chemical stimuli is similar to that reported for *fac*-[Re(CO)₃(dpknp)Cl] and studies are in progress to explore the thermodynamics and kinetics of the interconversion between the high- and low-energy forms of *fac*-[Re(CO)₃(dpkdnph)Cl] and its use as a spectrophotometric sensor.

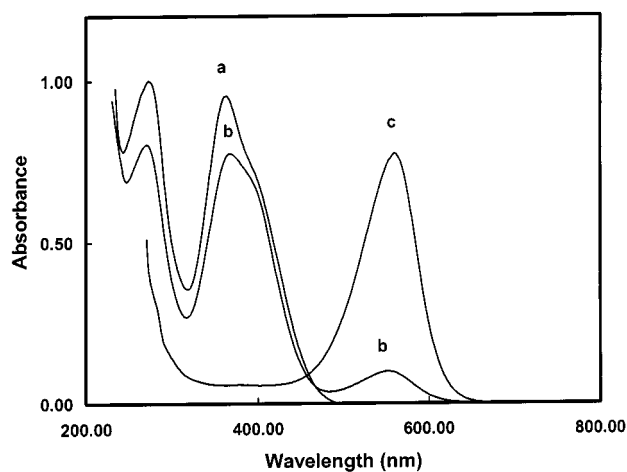


Figure 1. Electronic absorption spectrum of *fac*-[Re(CO)₃(dpkdnph)Cl] in: (a) CH₂Cl₂ (3.00×10^{-5} M); (b) CH₃CN (3.00×10^{-5} M); (c) DMF (1.00×10^{-5} M)

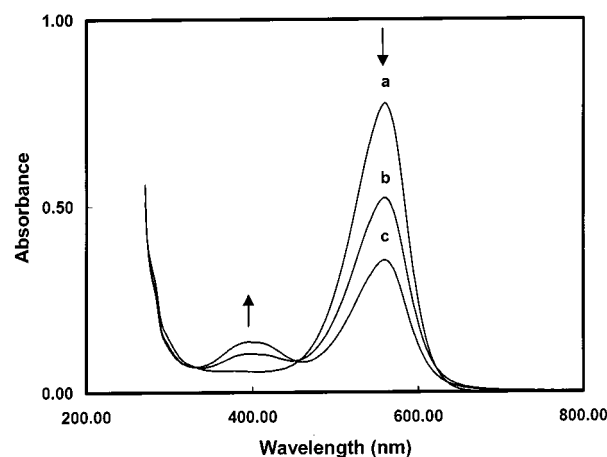


Figure 2. Electronic absorption spectrum of *fac*-[Re(CO)₃(dpkdnph)Cl] in DMF (1.00×10^{-5} M) (a) in the absence of sunlight, (b) after 3 h of sunlight exposure and (c) after 6 h of sunlight exposure

The electrochemical properties of *fac*-[Re(CO)₃(dpkdnph)Cl] in non-aqueous media were investigated using voltammetric techniques. Cyclic voltammograms of *fac*-[Re(CO)₃(dpkdnph)Cl] in DMF are shown in Figure 3. In these voltammograms rich redox processes appeared. The first reduction wave at $E_{p,c} = -0.76$ V is one-electron and irreversible. Scan rate variations on this wave from 100–2000 mV/s revealed no sign of reversibility pointing to structural/chemical modification following the first electronic transfer. Two quasi-reversible reduction waves appeared at $E_p = -1.24$ V ($E_{p,c} = -1.29$ and $E_{p,a} = -1.18$ V) and -1.62 V ($E_{p,c} = -1.75$ and $E_{p,a} = -1.48$ V) pointing to the stability of the electrochemically generated species following the second and third electron transfer. The quasi-reversible reduction wave at -1.62 V is assigned to the Re^{I/0} couple as it

falls in the potential range observed for such a couple in a variety of rhenium compounds of polypyridyl-like ligands of the type *fac*-[Re(CO)₃(L-L)Cl], where L-L = dpk, dpk.oxime, dpknpH and others.^[17–20] The irreversible oxidation wave at $E_{p,a} = +1.74$ V carries a peak current larger than that observed for the first irreversible reduction wave and points to its multi-electron character. The peak potential of this wave and its multi-electron character is similar to that reported for *fac*-[Re(CO)₃(dpk.oxime)Cl] and suggests a metal-mediated oxidation of coordinated dpkdnph.^[19] Electrochemically generated product waves appeared at $E_{p,a} = -1.62, +0.15, +0.55$ and $+0.98$ V pointing to structural modifications following electron transfer(s). Their appearance, coupled with the reversibility of the reduction waves, points to the formation of electrochemically generated transient intermediates sensitive to their surroundings that can be used to explore the electrochemical behaviour of various substrates toward *fac*-[Re(CO)₃(dpkdnph)Cl] in a procedure similar to that reported for *fac*-[Re(CO)₃(dpk)Cl].^[17,18]

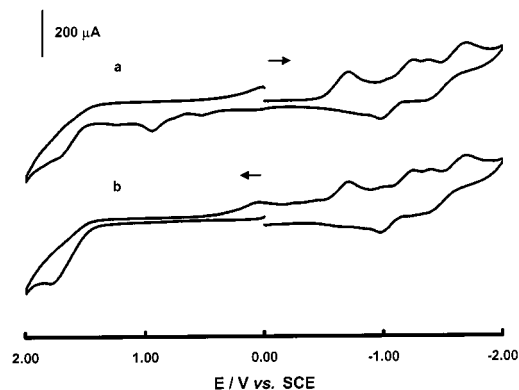


Figure 3. Cyclic voltammograms of *fac*-[Re(CO)₃(dpkdnph)Cl] in DMF solutions 0.1 M in [N(nBu)₄](PF₆) at a glassy carbon working electrode at a scan rate of 400 mV s⁻¹ vs. SCE

Single crystals of *fac*-[Re(CO)₃(dpkdnph)Cl]·CH₃CN were grown from an acetonitrile solution of *fac*-[Re(CO)₃(dpkdnph)Cl] and the structure was determined using X-ray crystallography. An ORTEP drawing of *fac*-[Re(CO)₃(dpkdnph)Cl]·CH₃CN (Figure 4) shows well separated linear CH₃CN and pseudo-octahedral *fac*-[Re(CO)₃(dpkdnph)Cl]. The distortion from an octahedral geometry about rhenium is due to the *N,N*-bidentate binding of dpkdnph and the formation of a six-membered metallacyclic ring (Re1–N1–C15–C00–C25–N5) in a boat conformation with the pyridine rings in a butterfly (Δ) formation. The N–N bite angle [N(1)–Re1–N(2)] of 83.03(11)° is of the same order as the 84.6° bite angles observed for the dpkO,OH in [ReOCl₂(dpkO,OH)],^[23] and is larger than the 74.3° reported for bipy in *fac*-[Re(CO)₃(bipy)(OPOF₂)].^[24] These results reveal that the six-membered metallacyclic ring in rhenium compounds with polypyridyl-like ligands is less constrained than the five-membered metallacyclic ring in rhenium compounds with α -diimine ligands. The 2,4-dinitrophenylhydrazine moiety

is planar with all nitrogen and carbon atoms sp² hybridized. The bond lengths and angles (Table 1) of the coordinated atoms are normal and similar to those reported for a variety of rhenium compounds of the type *fac*-[Re(CO)₃(N-N)X], where N-N = α -diimine ligand and X = anion.^[24–26]

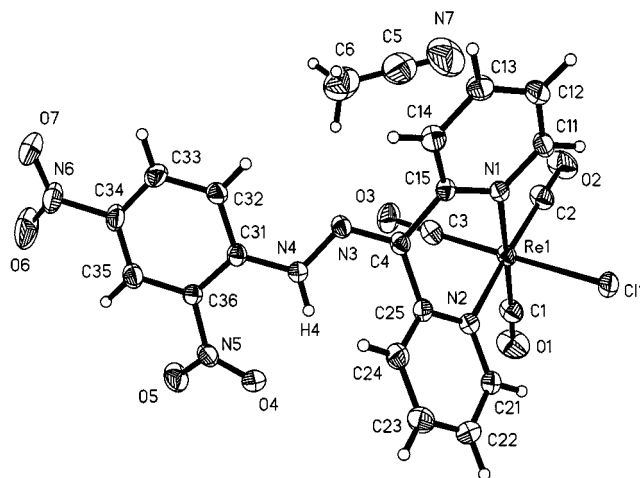


Figure 4. ORTEP drawings of the structure of *fac*-[Re(CO)₃(dpknpH)Cl]·CH₃CN; thermal ellipsoids are drawn at the 30% probability level

Table 1. Bond lengths [Å] and angles [°] for *fac*-[Re(CO)₃(dpkdnph)Cl]·CH₃CN

Re(1)–C(3)	1.900(4)	C(3)–Re(1)–C(1)	89.73(18)
Re(1)–C(1)	1.909(4)	C(1)–Re(1)–C(2)	90.61(17)
Re(1)–C(2)	1.924(4)	C(3)–Re(1)–N(2)	94.66(14)
Re(1)–N(2)	2.187(3)	C(1)–Re(1)–N(2)	91.94(15)
Re(1)–N(1)	2.210(3)	C(2)–Re(1)–N(2)	175.43(15)
Re(1)–Cl(1)	2.4732(11)	C(1)–Re(1)–N(1)	174.87(15)
C(2)–O(2)	1.138(5)	N(2)–Re(1)–N(1)	83.10(11)
C(3)–O(3)	1.151(5)	N(1)–Re(1)–Cl(1)	85.09(8)
C(1)–O(1)	1.142(5)	O(2)–C(2)–Re(1)	179.0(4)
C(4)–N(3)	1.298(5)	O(3)–C(3)–Re(1)	178.4(4)
C(4)–C(25)	1.488(5)	O(1)–C(1)–Re(1)	176.4(4)
N(3)–N(4)	1.351(4)	N(3)–C(4)–C(15)	114.8(3)
N(4)–C(31)	1.368(4)	N(3)–C(4)–C(25)	124.9(3)
N(5)–O(5)	1.213(4)	C(4)–N(3)–N(4)	118.6(3)
N(5)–O(4)	1.228(4)	O(5)–N(5)–O(4)	123.1(3)
N(6)–O(6)	1.203(6)	O(6)–N(6)–O(7)	124.9(4)
N(6)–O(7)	1.240(6)	N(7)–C(5)–C(6)	177.2(10)

The packing of molecules (Figure 5) shows *anti*-parallel *fac*-[Re(CO)₃(dpkdnph)Cl]·CH₃CN units interlocked via a network of non-covalent interactions that include hydrogen bonding of the type X···H–C, where X = O, N or Cl and oxygen-nitrogen charge-transfer between the *ortho*-nitro groups of adjacent molecules. Selected views of the non-covalent interactions are shown in Figure 6 and their bond angles and distances are listed in Table 2. The amide (NH) proton of the hydrazone backbone forms an intramolecular classical hydrogen bond of the type N–H···O with the oxygen atom (O4) of the *ortho*-nitro group. The acetonitrile

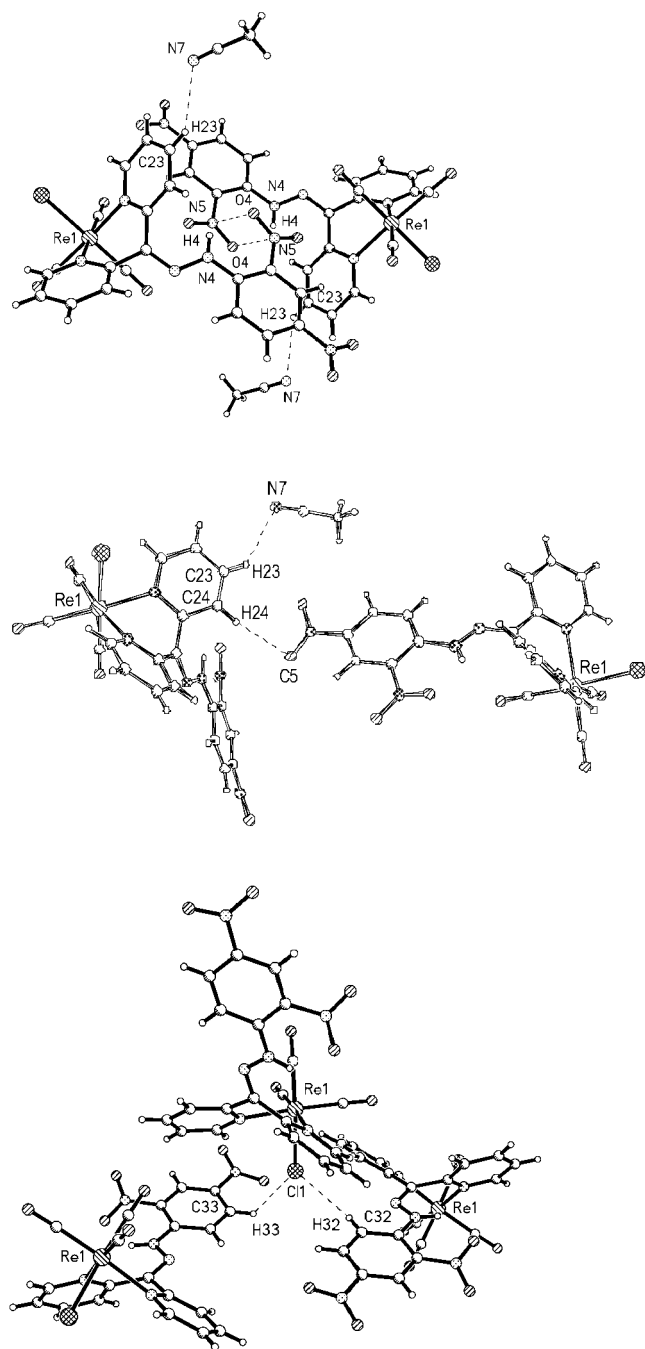


Figure 6. Selected views of the non-covalent bonding in the packed structure of *fac*-[Re(CO)₃(dpkdnph)Cl]·CH₃CN; non-covalent bonds are indicated by dashed lines

molecule binds to the adjacent proton (Figure 6b), whereas the *p*-nitro group binds to an adjacent *fac*-[Re(CO)₃(dpkdnph)Cl] unit and the axial chloride doubly bridges two adjacent phenyl rings in a [C(32)–H(32)···Cl(1)···H(33)–C(33)] bonding form (Figure 6c). The bond lengths and angles of the non-covalent interactions are of the same order as those reported for a variety of compounds containing such bonds.^[27–29] The difference in the oxygen–nitrogen bond length (Table 1) of the *para*-nitro group hints to an increase in electron density

around the oxygen atom participating in the non-covalent C(24)–H(24)···O(6) interaction.

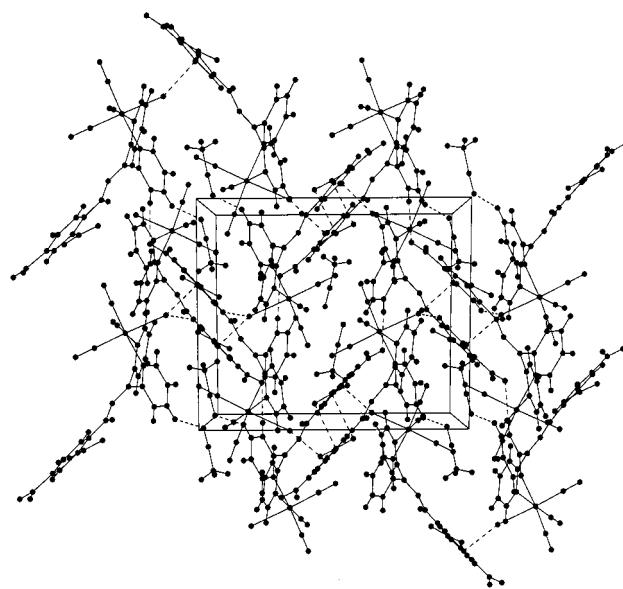


Figure 5. Packing of the molecules of *fac*-[Re(CO)₃(dpkdnph)Cl]·CH₃CN in the unit cell; non-covalent bonds are indicated by dashed lines

Table 2. Bond lengths [Å] and angles [°] of the non-covalent interactions in the packed structure of *fac*-[Re(CO)₃(dpkdnph)Cl]·CH₃CN

Bond ^[a]	Distance	Angle
O(4)···H(4)–N(4)	2.647	126.7
O(6)···H(24)–C(24) ⁽¹⁾	2.450	166.3
N(7)···H(23)–C(23) ⁽²⁾	2.609	136.1
Cl(1)···H(32)–C(32) ⁽³⁾	2.790	146.7
Cl(1)···H(33)–C(33) ⁽⁴⁾	2.853	120.1
N(5)–O(4)···N(5)–O(4) ⁽⁵⁾	2.954	99.4, 80.6

^[a] Symmetry transformations used to generate equivalent atoms: (1): $1/2 - x, 1/2 + y, 3/2 - z$; (2): $-1/2 + x, 1/2 - y, 1/2 + z$; (3): $-1/2 + x, 1/2 - y, -1/2 + z$; (4): $3/2 - x, 1/2 + y, 3/2 - z$; (5): $1 - x, -y, 2 - z$.

Owing to their convenient synthesis, rich physicochemical properties and potential use as molecular sensors, work is in progress to explore the electro-optical properties, solid state structures and solution conformations of a variety of di(2-pyridyl) ketone derivatives and their rhenium compounds.

Experimental Section

Reagents and Reaction Procedures: Solvents were reagent grade and thoroughly deoxygenated prior to use. All other reagents were obtained from commercial sources and used without further purification. All reactions were performed under a nitrogen atmosphere.

Physical Measurements: Electronic absorption spectra were recorded on a Perkin–Elmer Lambda 19 UV/Vis/NIR spectrometer. Solution ^1H NMR spectra were recorded on a Bruker ACE 200-MHz Fourier transform spectrometer and referenced to the residual protons in the deuterated solvent. Infrared spectra were recorded as KBr pellets on a Perkin–Elmer Spectrum 1000 FT-IR Spectrometer. Photochemical measurements were conducted on deoxygenated solutions before and after exposure to sunlight. Electrochemical measurements were performed with the use of a Princeton Applied Research (PAR) Model 173 potentiostat/galvanostat and Model 276 interface in conjunction with a 286 PC. Data were acquired with the EG&G PARC Headstart program and manipulated using Microsoft Excel Program. Measurements were performed in solutions that were 0.1 M in $[\text{N}(n\text{Bu})_4](\text{PF}_6)$. The $E_{\text{p,a}}$, $E_{\text{p,c}}$ and $E_{\text{p}} = (E_{\text{p,a}} + E_{\text{p,c}})/2$ values were referenced to the potassium chloride saturated calomel electrode, SCE, at room temperature and are uncorrected for junction potentials. The number of electrons in the redox waves was determined using the oxidative peak current of the reversible one electron $\text{FeCp}_2/\text{FeCp}_2^+$ couple as an internal standard. Electrochemical cells were of conventional design based on scintillation vials or H-cells. A glassy-carbon disc was used as the working electrode and Pt-wire as a counter electrode.

Analytical Procedures: Microanalyses were performed by MEDAC Ltd., Department of Chemistry, Brunel University, Uxbridge, United Kingdom.

Preparation of dpkdnph: A mixture of dpk (200 mg, 1.09 mmol), 2,4-dinitrophenylhydrazine (220 mg, 1.12 mmol), ethanol (100 mL) and conc. HCl (0.25 mL) was refluxed for 5 h. The resulting reaction mixture was allowed to stand at room temperature for 3 h. A yellow solid was filtered off, washed with diethyl ether, hexane and dried; yield 350 mg, 0.96 mmol (88%). $\text{C}_{17}\text{H}_{12}\text{N}_6\text{O}_4$ (364.3): calcd. C 56.04, H 3.33, N 23.06; found C 55.86, H 3.32, N 22.98. IR (KBr disk): $\nu(\text{N}-\text{H})$ 3320 cm^{-1} . The low solubility of dpkdnph in polar and non-polar solvents prevented any solution measurements on this compound.

Preparation of *fac*-[Re(dpknph)(CO)₃Cl]: A mixture of $[\text{Re}(\text{CO})_5\text{Cl}]$ (200 mg, 0.55 mmol), dpkdnph (250 mg, 0.67 mmol) and toluene (50 mL) was refluxed for 20 h. The resulting mixture was allowed to cool to room temperature and reduced in volume to \approx 25 mL. A yellow solid was filtered off, washed with hexane and diethyl ether, and dried; yield 300 mg, 0.45 mmol (82%). $\text{C}_{20}\text{H}_{12}\text{ClN}_6\text{O}_7\text{Re}$ (670.0): calcd. C, 35.87, H 1.80, N 12.54; found C 35.91, H 1.91, N 12.48. IR (KBr disk): $\nu(\text{C}=\text{O})$ 2020, 1900, 1890 cm^{-1} , $\nu(\text{NO}_2)$ 1340, $\nu(\text{N}-\text{H})$ 3273. ^1H NMR ($[\text{D}_6]\text{DMSO}$): δ = 11.80 (s, 1 H, NH), 9.15 (d, 1 H, dnph), 8.95 (d, 1 H, dnph), 8.85 (s, 1H dnph), 8.50–8.00 (closely spaced overlapped triplets and doublets, 6 H, dpk), 7.8 (overlapped triplets, 2 H, dpk). In CDCl_3 : δ = 11.98 (s, 1 H, NH), 9.40 (d, 1 H, dnph), 9.16 (s, 1 H, dnph), 9.14 (d, 1 H, dnph), 8.45 (d, 1 H, dpk), 8.25–8.10 {overlapped triplet (8.16) and doublet (8.15), 2 H, dpk}, 8.04 (t, 1 H, dpk), 7.85 (d, 2 H, dpk), 7.65 (t, 1 H, dpk), and 7.55 (t, 1 H, dpk). UV/Vis $\{\text{CH}_2\text{Cl}_2, \text{nm}(\epsilon)\}$: 396 sh (28,700); 358 (37,600), 268 (39,400).

X-ray Crystallography: When *fac*- $[\text{Re}(\text{CO})_3(\text{dpkdnph})\text{Cl}]$ was allowed to stand in acetonitrile solution for several days brown cubic crystals of *fac*- $[\text{Re}(\text{CO})_3(\text{dpkdnph})\text{Cl}]\cdot\text{CH}_3\text{CN}$ were obtained. A single crystal was selected and mounted on a glass fibre with epoxy cement. A Bruker diffractometer equipped with a Mo- K_α radiation source and a graphite monochromator was used for data collection, and the SHELXTL software package version 5.1 was used for structure solution. Cell parameters and other crystallographic information are given in Table 3 along with additional details con-

cerning data collection.^[30–32] The location of the rhenium atom was determined from a Patterson map, and the remaining non-hydrogen atoms were located in subsequent difference Fourier maps. All non-hydrogen atoms were refined with anisotropic thermal parameters. In the final least-squares cycle, 344 parameters were fitted to 4095 observations, for a data to parameters ratio of 11.90:1. The least-squares residuals and other relevant parameters are given in Table 3.

Table 3. Crystal data and structure refinement for *fac*- $[\text{Re}(\text{CO})_3(\text{dpkdnph})\text{Cl}]\cdot\text{CH}_3\text{CN}$

Empirical formula	$\text{C}_{22}\text{H}_{15}\text{ClN}_7\text{O}_7\text{Re}$
Formula mass	711.06
Temperature	298(2) K
Wavelength	0.71073 Å
Crystal system	Monoclinic
Space group	$P2_1/n$
Unit cell dimensions	$a = 12.1221(19)$ Å, $\alpha = 90^\circ$ $b = 14.226(2)$ Å, $\beta = 98.691(13)^\circ$ $c = 14.6170(19)$ Å, $\gamma = 90^\circ$
V	2491.7(7) Å ³
Z	4
Density (calculated)	1.895 mg/m^3
Absorption coefficient	5.042 mm^{-1}
$F(000)$	1376
Theta range for data collection	2.01 to 25.00 °
Reflections collected/unique	8326/4095 [$R(\text{int}) = 0.0417$]
Completeness to theta: 25.00	93.2%
Absorption correction	Empirical
Max. and min. transmission	0.3158 and 0.2749
Refinement method	Full-matrix least-squares on F^2
Data/restraints/parameters	4095/0/344
Final R indices [$I > 2\sigma(I)$]	$R1 = 0.0227$, $wR2 = 0.0547$
R indices (all data)	$R1 = 0.0294$, $wR2 = 0.0568$
Largest diff. peak and hole	0.646 and $-0.695 \text{ e}\cdot\text{Å}^{-3}$

Acknowledgments

I acknowledge funding from the following: The University of the West Indies (UWI), Inter-America Development Bank (IDB) for funds to establish the X-ray laboratory at UWI-Mona.

- [1] L. R. Sutton, A. J. Blake, W.-S. Li, M. Schröde, *J. Chem. Soc., Dalton Trans.* **1998**, 279–284.
- [2] F. Pan, C. Bosshard, M. S. Wong, C. Serbutoviez, K. Schenk, V. Gramlich, P. Gunter, *Chem. Mater.* **1997**, *9*, 1328–1334.
- [3] A. S. Batsanov, A. V. Churakov, M. A. M. Easson, L. J. Govenlock, J. A. K. Howard, J. M. Moloney, D. Parker, *J. Chem. Soc., Dalton Trans.* **1999**, 323–330.
- [4] J. Frelek, J. Jagodzinski, H. Meyer-Figge, W. S. Sheldrick, E. Wieteska, W. J. Szczepek, *Chirality* **2001**, *13*, 313–321.
- [5] A. Bacchi, A. Bonini, M. Carcelli, F. Ferraro, E. Leporati, C. Pelizzi, G. Pelizzi, *J. Chem. Soc., Dalton Trans.* **1996**, 2699–2704.
- [6] D. Armesto, A. Ramos, M. J. Ortiz, W. M. Horspool, M. J. Mancheno, O. Caballero, E. P. Mayoral, *J. Chem. Soc., Perkin Trans. 1* **1997**, 1535–1542.
- [7] T. Odashima, M. Yamaguchi, H. Ishii, *Talanta* **1995**, *42*, 1229–1237.
- [8] R. Hai-Ying He, X.-K. Jiang, *J. Phys. Org. Chem.* **1999**, *12*, 392–400.
- [9] M. R. Maurya, S. Khurana, C. Schulzke, D. Rehder, *Eur. J. Inorg. Chem.* **2001**, 779–788.

- [10] J. G. March, B. M. Simonet, F. Grases, *Analyst* **1999**, 897–900.
- [11] D. Enders, R. Peters, R. Lochman, G. Raabe, J. Runsink, J. W. Bats, *Eur. J. Org. Chem.* **2000**, 3399–3426.
- [12] V. Atlan, H. Bienaymé, L. El Kaim, A. Majee, *Chem. Commun.* **2000**, 1585–1586.
- [13] A. Carbayo, J. V. Cuevas, G. García-Herbosa, S. García-Granda, D. Miguel, *Eur. J. Inorg. Chem.* **2001**, 2361–2363.
- [14] J. F. Hartwig, *Angew. Chem. Int. Ed.* **1998**, *37*, 2090–2093.
- [15] C. Bosshard, K. Sutter, P. Pretre, J. Hullinger, M. Florsheimer, P. Kaatz, P. Gunter, *Organic Nonlinear Optical Materials*; Gordon and Breach Science Publishers, Amsterdam, **1995**.
- [16] *Molecular Nonlinear Optics: Materials, Physics, Devices* (Ed.: J. Zyss), Academic Press, Boston, **1994**.
- [17] M. Bakir, J. A. M. McKenzie, *Electroanal. Chem.* **1997**, *425*, 61–66.
- [18] M. Bakir, J. A. M. McKenzie, *J. Chem. Soc., Dalton Trans.* **1997**, 3571–3578.
- [19] M. Bakir, *J. Electroanal. Chem.* **1999**, *466*, 60–66.
- [20] M. Bakir, K. Abdur-Rashid, *Transition Met. Chem.* **1999**, *24*, 384–388.
- [21] M. Bakir, K. Abdur-Rashid, W. H. Mulder, *Talanta* **2000**, *51*, 735–741.
- [22] *Tables of Spectral data for Structure Determination of Organic Compounds* (Eds.: F. L. Boschke, W. Fresenius, J. F. K. Huber, E. Pungor, G. A. Rechnitz, W. Simon, Th. S. West), Springer-Verlag, Berlin Heidelberg, **1983**.
- [23] T. I. A. Gerber, H. J. Kemp, J. G. H. du Preez, G. Bandoli, *J. Coord. Chem.* **1993**, *28*, 329–336.
- [24] E. Horn, M. R. Snow, *Aust. J. Chem.* **1980**, *33*, 2369–2376.
- [25] W.-M. Xue, M. C.-W. Chan, Z.-M. Su, K.-K. Cheung, S.-T. Liu, C.-M. Che, *Organometallics* **1998**, *17*, 1622–1630.
- [26] V. W.-W. Yam, K.-Z. Wang, C.-R. Wang, Y. Yang, K.-K. Cheung, *Organometallics* **1998**, *17*, 2440–2446.
- [27] D. Braga, F. Grepioni, G. R. Desiraju, *Chem. Rev.* **1998**, *98*, 1375–1405.
- [28] J. P. Glusker, M. Lewis, M. Rossi, *Crystal Structure Analysis for Chemists and Biologists*, Wiley-VCH, New York, **1994**.
- [29] J. H. Williams, *Acc. Chem. Res.* **1993**, *26*, 593–598.
- [30] Bruker-SHELXTL (1997). Software Version 5.1. Bruker AXS, Inc., Madison, Wisconsin, U.S.A.
- [31] Bruker-XSCANS (1996). Software Version 2.2. Bruker AXS, Inc., Madison, Wisconsin, U.S.A.
- [32] G. M. Sheldrick, SHELX-97 and SHELXL-97, University of Göttingen, Germany, **1997**.

Received September 10, 2001
[101359]